Indian Journal of Pure & Applied Physics
Vol. 63, October 2025, pp. 930-944
DOI: 10.56042/ijpap.v63i10.19539

Economic Emission Load Dispatch with Renewable Energy and Electric Vehicle Integration: A Real-Data Approach Using Equilibrium Optimizer

Jatin Soni[a*] & Kuntal Bhattacharjee[b]

[a]School of Electrical Engineering, Shri Mata Vaishno Devi University, Katra 182 320, India

[a,b]Institute of Technology, Nirma University, Ahmedabad, Gujarat 382 481, India

Received: 8th May 2025 ; accepted:25th August 2025

This paper presents an optimized solution to the Wind-Solar Plug-in Electric Vehicle Dynamic Economic Emission Load Dispatch (WSPEV DEELD) problem using the Equilibrium Optimizer (EO) algorithm. Real-world data from the renewable. Ninja platform for Gujarat, India, is used to handle uncertainties related to the underestimation and overestimation of wind and solar power, as well as PEV arrival, departure, and waiting times. EO's balance between exploration and exploitation helps minimize generation cost and emissions while ensuring sustainability. Simulations consider Vehicle-to-Grid (V2G) and Grid- to-Vehicle (G2V) interactions using real-time RES data and PEV behavior. The results show improved system performance and demonstrate that the EO algorithm provides a robust, feasible strategy for dynamic RES and PEV integration into the power grid. Com- parisons with other recent methods confirm EO's effectiveness in solving complex power dispatch problems under real-world constraints.

Keywords: Wind-Solar plug-in electric vehicle (WSPEV), Dynamic economic emission load dispatch (DEELD), Equilibrium optimizer (EO), Renewable energy sources (RES), Plug-in electric vehicles (PEVs), Power system integration

1 Introduction

Since PEVs operate cleaner than conventional fuel-based cars, they provide a significant potential to reduce pollutant emissions, making them a recent trend in contemporary transportation[1]. Despite the fact that the trend is encouraging, the widespread use of PEVs presents additional difficulties for the stability of the electrical system. As the number of PEVs rises, so does the power supply needed for everyday travel, leading to conflicts between PEV charging loads and conventional power needs[2]. In this regard, there should be a coordinated strategy that focuses on reducing such conflicts and ensuring reliable system operation. The actual user travel behavior greatly varies, showing a massive fluctuation within the power system[3]. Consequently, as the demand for electricity increases, more power has to be generated, and the generation units are strained to highest operational requirements[4]. Electricity is one of the cornerstones of the modern world; it is one of the most global infrastructures in the world, and therefore, efficient generation and transmission require the technical and economic power generation[5]. As electric power is generated using very costly resources, there is the need to optimize power generation while keeping overall cost levels at the lowest ends.

The Economic Load Dispatch (ELD) problem formulates the optimum power generation by generators in a system to meet the demand by minimizing the generation cost considering all system constraints[6]. In this, a variation of the problem has come up as the Economic Emission Load Dispatch (EELD), in which emission constrains are also taken into account to minimize the environmental impact[7]. The aim is to have minimum generation cost but keep the emissions within allowable limits since sustainability and environmental regulations are becoming more prominent in power system planning. Dynamic EELD (DEELD) is an extension of the above problems where demand for power is time varying, and Renewable Energy Sources (RES) such as wind and solar power are incorporated[8]. DEED is a more complex problem because the RES exhibits uncertainty and variability. This has further complexity for power grid as PEVs work as an energy consumer as well as potential supplier through Vehicle-to-Grid interaction Qiao *et al.* (2025)[9], D. Zou, Ma, Li, Ouyang, and Shao (2025). For the case of PEVs, the charging and discharging patterns

*Corresponding author: E-mail: sonijatin1995@gmail.com

again have similar conditions, and proper control is in need in order to have stability and reliability in the distribution grid. Metaheuristic algorithms have been broadly employed to address such complexities since they efficiently solve difficult non-linear problems. Therefore, Metaheuristics used to improve equilibrium between exploration and exploitation and are less prone than previous methods to get trapped in local optima[10].

1.1 Literature Survey

The penetration of RES and PEVs into traditional generation systems gives rise to new challenges and opportunities in ELD as well as EELD. Recent works manifest that a great variants of optimization methods have been applied to handle challenges. Bhattacharjee *et al*. (2017) optimized real-time DEELD by applying dynamic programming[11]. The method is mainly designed for the traditional generation power system without accounting for RES and PEVs; therefore, not truly relevant in a modern grid sense. Basu *et al*. (2016) extended ELD models considering RES with the help of metaheuristic algorithms like GA and PSO[12]. Though it has proven efficient, the same models have struggled to accurately capture RES-variations in character, as it is intermittent. Fauziyah *et al*. (2023) demonstrated the incorporation of RES into DEELD with the help of MILP[13]. The method is mathematically sound but fails to deal with uncertainties related to the generation of RES which under-estimates its practical applicability. Ma *et al*. (2017) Studied the integrated RES and PEVs with ELD[14]. A hybrid approach that included PSO and Monte Carlo simulation to estimate the cost is proposed; however, involvement of several variables hiked the computational complexity of it. Qu *et al*. (2017), Chen *et al*. (2017) and Qu *et al*. (2017) proposed a model that incorporated wind and solar along with EELD. Optimization was carried out by Simulated Annealing and Dynamic Programming Qu, Qiao, Zhu, Jiao, *et al*. (2017)[15]. Major drawback is it has not considered the constraints of PEV arrival and departure. Yan *et al*. (2022) study's primary aim was optimizing EED, taking into consideration wind- solar and plug-in Electric Vehicle (PEVs) integration using a Harmony Search Algorithm coupled with fuzzy logic Yan *et al*. (2022). However, the model was proved to underpredict with low precision regarding the cost estimates of RES.

In Zou *et al*. (2022), the EED model was extended with PEV arrival and departure constraints[16]. It addressed the problem with multi-objective optimization and applied game theory for the equilibrium. The multi-objective optimization problem is complex in terms of designing appropriate weighting factors. Qiao *et al*. (2022) considered the impact of cost estimation accuracy on EED by using neural networks to perform the cost estimation and evolutionary algorithms for optimization[17]. Its limitation is the need for high-quality training data in order to have good performance with the neural networks. In Chen *et al*. (2020), Markov Chain models were used to analyze equilibrium optimization with PEV arrival and departure constraints in DEELD[18]. Although uncertainty is effectively handled, high computational costs are maintained in large-scale systems. In Mei *et al.* (2019) study, the advantages of wind-solar and PEVs are assessed by means of OPF algorithms and life cycle analysis for cost estimation. Although this method is not scalable for large-scale power systems[19].

Rajani *et al*. (2021) discussed grid constraints' impact on EED with integration of wind-solar and PEVs[20]. Real-time optimization was achieved with the use of MPC and sensitivity analysis. Due to not considering dynamic grid constraints fully, the optimization accuracy cannot be achieved in full sense. In 2022, Yan *et al.* and Zou *et al*. used a decentralized approach for EED under combined integration of wind-solar and PEVs using game theory and decentralized optimization algorithms. Convergence and global optimality are still yet to be assured in a decentralized setup[21,22]. Nourianfar *et al*. (2022) applied MCDM and sensitivity analysis to find the compromise between economic benefits and environmental impact in dynamic dispatch with wind-solar, and PEVs[23]. One of the significant drawbacks of MCDM is that weights are assigned subjectively for the criteria. Qiao *et al*. (2022) used the spatial distribution of wind-solar resources and PEV demand using Geographic Information System techniques for spatial modeling[24]. Its effectiveness is reduced with the availability of spatial data for RES and with less accuracy. In Shevchenko *et al*. (2017), Regulatory policy analysis along with the optimization modelling approach is challenging while quantification of policy uncertainties in the optimization framework itself is tough Shevchenko (2017).

Goel *et al*. (2018) has developed an approach based on battery swapping that maximized the profit of charging stations using the concept of Multi-band robust optimization[24]. The major drawback is that the high up-front installation cost and low willingness of consumers. Kang *et al*. (2016) have developed a centralized charging strategy and scheduling algorithm for battery swapping[25]. A major challenge in the real-world implementation is coordination with various stakeholders and infrastructure constraints. Gao *et al*. (2019) applied game theory and decentralized optimization to manage charging stations[26]. With this assumption, the rational behavior with perfect information assumption of Electric Vehicle Charging Stations (EVCSs) is unlikely to prevail in real life. Moghaddam *et al.* (2018) successfully reduces travel time and charging cost in Coordinated Dynamic Pricing Model Moghaddam, Ahmad, Habibi, and Masoum (2019). PEV users resist changing their charging behavior and rely on a huge penetration rate.

In recent years, the DEED incorporating PEVs (DEED-PEV) has received more attention. Zhang *et al*. examined PEV charging and discharge[27]. They successfully smoothed the power needs by using shaving of peak and trough fills. While valley filling is used to split the charging loads, peak shaving is utilized to distribute the PEVs' discharging power. As a result, power load fluctuations are greatly decreased. Zhang *et al.* concurrently considered the charging preferences of PEV users and the advantages of energy demand control in their study of nine DEED-PEV problems with various PEV charging and discharging scenarios[28]. Behera *et al*. looked at the effects of G2V loads and V2G supports on DEED-PEV[29]. They used V2G power and G2V demand management to save emissions and operating expenses. Al-Bahrani *et al*. investigated the DEED-PEV under a few real-world operational power constraints related to both inequality and equality[30]. Peak shaving and valley filling areas employ PEV load demand management.

Wind and solar energy are plentiful, unadulterated, and easy to harvest in nature. The most useful RES are acknowledged to be these. They've been employed extensively in the field of electricity. A significant quantity of electric power will be available for both conventional loads and PEVs thanks to the wind turbine's ability to convert wind energy into electrical energy and the solar panels' ability to do the same. In the last 10 years, DEED PEV has included solar and/or wind energy. Basak *et al*. used Strength Pareto Evolutionary Algorithm 2 (SPEA2) to provide a unique flexibility-based probabilistic ED issue utilizing wind power in F Chen *et al*. (2017). The multi-objective evolutionary algorithm based on decomposition (MOEA/D) was utilized by Basak *et al*. assessed the unpredictable properties of wind energy using a DEED model with wind power[31].

Another approach has been proposed in the scope of the multi-area DEED model, which additionally considers the interaction of hydro-wind-thermal power systems[32]. The authors utilized a technique called self-adaptive multi-objective differential evolution, or SaMODE. Wind energy units were included into the DEED-PEV in 2021, and Zou *et al*. proposed a new framework for combining wind power with PEVs. The authors used the PEVs' charging and discharging phases to balance the penalty cost that resulted from overestimating (OE) and underestimating (UE) the amount of wind power that was available[33]. Qiao and Liu's unique integrated framework of wind farms and electric vehicles Qiao and Liu (2020) employed electric car charging and discharging to offset the extra cost involved with the exaggerated and underrated available wind power. WSPEV DEELD are Wind-Solar PEVs developed by Soni *et al*. to reduce the expense of wind-thermal electricity and the emission of pollutants[34-36]. To add a little realism to the energy system, they added some quadratic limitations. According to the previously described factors, previous theoretical models often come off as utopian and oversimplified, falling short in addressing the real-world energy consumption situations, especially in industrial settings. Furthermore, the majority of current methods are based on ideal theoretical presumptions. This emphasizes the need for more reliable approaches that take into account practical considerations like PEVs, wind, and solar energy. As a result, a new model is put forward that takes into account actual data for RES, their UE and OE costs, and the arrival, departure, and waiting durations of PEVs. This model may be successfully resolved by using sophisticated optimization techniques.

1.2 Research Novelties

This research introduces several key innovations in solving the WSPEV DEELD problem by integrating real-world data and uncertainties related to RES and PEVs. A novel optimization method, the EO, is applied to address these complexities, ensuring more efficient and realistic power dispatch solutions. Key novelties of the research include advanced uncertainty modeling, handling PEV constraints, and performance comparisons with existing algorithms.

i This research provides a pioneering approach to integrate Wind, Solar, and PEVs into the DEELD model. By addressing the complex interactions between RES and PEVs, the model offers an advanced solution for optimizing power dispatch while considering emission reduction. This integration is particularly novel because it focuses on managing dynamic scenarios that occur in modern power systems with increasing RES penetration.

ii Because it improves the WSPEV DEELD model's accuracy and efficiency, the implementation of the EO approach is a noteworthy addition to the area. EO is known for its strong optimization capabilities, making it ideal for handling the multi-dimensional complexities of RES and PEV integration in ELD. By leveraging EO, the model is able to find optimal power dispatch solutions more effectively than traditional methods.

iii The model tackles the often-overlooked issue of UE and OE in wind and solar power generation. By addressing these errors, the model increases its robustness and reliability, ensuring that power systems can handle variations in energy production under different environmental conditions.

iv key advancement of this research is the inclusion of PEVs constraints, such as arrival, departure, and waiting times. This makes the model more applicable to real-world scenarios, where the timing and energy demands of PEVs must be considered for efficient power system management. The model may take into account the increasing number of electric cars in contemporary power networks thanks to the inclusion of PEV limitations.

The rest of the paper is organized as follows: The DEED-PEV mathematical formulation with all limitations is shown in Section 2. We will provide the EO approach and the procedures to be followed to optimize WSPEV DEED issue in Section 3. The analysis and experimental findings of four scenarios involving 10 and 20 thermal producing units are presented in Section 4. The findings of this study are reported in Section 6.

2 WSPEV DEED Modeling

PEV charging and discharging processes are also random, and RES supplies like solar and wind power are unpredictable and sporadic Soni and Bhattacharjee (2022). Therefore, to manage the unpredictability and fluctuation of these resources, a more dynamic strategy is needed. To maximize power system performance in a power system with many generating units, a WSPEV DEED has been developed. In addition to economic and environmental goals, they might include PEVs, wind turbines, solar panels, and traditional thermal units. The following is the expression:

$$E_T = \sum_{i=1}^{N} \alpha_{iT} + \beta_{iT} T_{iT} + \gamma_{iT} T_{iT}^2 + \xi_{iT} \exp(\Upsilon_{iT} T_{iT}) \quad \ldots . (1)$$

The emission variables of the iT^{th} unit are specified by ξ_{iT} and Y_{iT}, whereas the emission variables of the iT^{th} unit have stated by α_{iT}, β_{iT}, and γ_{iT}. In this case, N represents the quantity of units, T is the deliver duration and emission variables, and T is the output power from thermal units. The overall price is given by taking into account the corresponding trade-off among the UE and OE of RES.

$$Minimize\ F_t = [(\chi F_T + (1-\chi) F_T] + F_W + F_S \ldots (2)$$

with F_T representing total cost by thermal units, F_W and F_S representing total price of wind and solar power with UE and OE. The weighting factor, χ, is used to transform multi-objective functions into single-objective ones.

$$F_T = \sum_{j=1}^{N} a_{iT} + b_{iT} T_{iT} + c_{iT} T_{iT}^2 + \eta_{iT} \sin[f_{iT}(T_{iT}^{min} - T_{iT})] \quad \ldots (3)$$

T_{imin}, T_{imax} are the lowest and most powerful obstacles of each generator; a_{iT}, b_{iT}, and c_{iT} are fuel cost variables of the iT th unit; and η_{iT} and f_{iT} are variables of the thermal iTth unit describing VPLE. Below is a mathematical calculation for the immediate expenses of wind unit[37].

$$F_W = \sum_{t=1}^{T}\left[\left\{\sum_{j=1}^{N_W} C_W \times P_{Wd,jt}\right\} + \left\{\sum_{j=1}^{N_W} K_{p,wd} \times (P_{Wj,av} - P_{Wd,jt})\right\} + \left\{\sum_{j=1}^{N_W} K_{r,wd} \times (P_{Wd,jt} - P_{Wj,av})\right\}\right] \quad \ldots (4)$$

where $P_{Wj,av}$ and $P_{Wd,jt}$ represent the jth wind unit's accessible and anticipated output power, respectively; C_W is the wind unit's cost pervasive and $K_{p,wd}$ and $K_{r,wd}$ are penalized factors associated with wind power's OE and undestimation; The whole cost of the solar unit Three elements affect the solar unit's overall cost: 1. Costing directly 2. The price of fines for not utilizing all of the power generated by photovoltaic cells. 3. The price of fines for generating less PV power than anticipated. A description of such a system is given below.

$$F_S = \sum_{t=1}^{T}\left[\left\{\sum_{k=1}^{N_S} C_{pv} \times P_{pv,kt}\right\} + \left\{\sum_{k=1}^{N_S} K_{p,pv} \times (P_{pv,av} - P_{pv,kt})\right\} + \left\{\sum_{k=1}^{N_S} K_{r,pv} \times (P_{pv,kt} - P_{pv,av})\right\}\right] \quad \ldots (5)$$

where $K_{p,pv}$ and $K_{r,pv}$ are penalty variables for undestimation and OE of solar power, respectively; C_{pv} is the cost steady for kth solar units of measurement; and $P_{pv,av}$ and $P_{pv,kt}$ are the accessible and derived power generated of k_{th} sunlight units, respectively.

2.1 Modeling of PEVs

PEV modeling is a very interesting topic for automobile companies, policy- makers, and researchers since it is closely associated with the excitement of PEVs' impact on energy consumptions, greenhouse gas emissions, among others[38-40]. PEV modeling may include a wide range of topics: for example, one can model battery performance, charging infrastructure, or consumer behavior. The following sign function can be applied to describe the process in PEVs:

$$\begin{cases} P_{ch,t} = Mark(x)\sum_{l=1}^{N_{pev}} P_{rv2g,l} & x < 0 \\ P_{ch,t}\ and\ P_{Dch,t=0} & x = 0 \\ P_{Dch,t} = Mark(x)\sum_{l=1}^{N_{pev}} P_{rv2g,l} & x > 0 \end{cases} \quad \ldots (6)$$

P_{cht} is the PEV's charging status, x<0, Mark(x)=-1, N_{v2g} is the quantity of PEVs, and Prv2g,l is maximum power rating of lth PEV. The charging status of PEV is marked as x > 0, Mark(x)=1, and $P_{Dch,\,t} > 0$, whereas x=0 is the optimum value of PEV.

2.2 Constraints

A number of limitations pertaining to the functionality and performance of the components may also exist in the WSPEV DEED model. The following are some examples of limitations that might be relevant to the WSPEV DEED dilemma:

2.2.1 Thermal Generator Operating Limit

The operational limit of a thermal generator is the highest amount of electricity that a thermal power plant is capable of producing. The basis for such a limitation is the plant's mechanical and thermal capacity[41,42]. The same operating constraint was developed to keep the plant's equipment safe and reliable while preventing damage.

$$T_i^{min} \le T_i \le T_i^{max}; i = 1,2,\ldots,N \quad \ldots (7)$$

$$0 \le w_{outj} \le w_{outr,j}; j = 1,2,\ldots,N_W \quad \ldots (8)$$

$$0 \le S_{outk} \le S_{outr,k}; k = 1,2,\ldots,N_S \quad \ldots (9)$$

In this case, $w_{outr,j}$ represents the maximum power that jth wind farms can generate, and $S_{outr,k}$ represents the maximum power that kth solar units can produce.

2.2.2 Constraint of Power Balance

The total power generated and utilized in a power system are ensured to be equal by a mathematical calculation called a power balance constraint.

$$\sum_{i=1}^{N} T_i + \sum_{k=1}^{N_W} W_{p,k} - (T_D + T_L) = 0 \quad \ldots (10)$$

The following formula is used to determine the total transmission loss:

$$T_L = \sum_{m=1}^{N}\sum_{n=1}^{N} T_m B_{mn} T_n + \sum_{m=1}^{N} B_{m0} T_m + B_{00} \quad \ldots (11)$$

The B matrix's components are B_{mn}, B_{m0}, and B_{00}.

2.2.3 Remain Power Constraint of PEVs

One of the constraints of a PEV's residual power limit is that it imposes a total amount of power extracted from a vehicle battery until the latter is completely depleted[42,43].

$$R_t = R_{t-1} + \{\delta_c P_{ch,kt}\} - \left\{\frac{1}{\delta_D} P_{Dch,kt}\right\} - R_{Trip,t} \quad \ldots (12)$$

where the PEVs' charging and discharging efficiency is represented by δ_c and δ_D. The power used by PEVs when discharging is shown by P_{Dch}, whereas P_{Ch} represents the power taken during charging. The following Sun, Yang, Ma, Ferr´e, and Yan (2020) offers the mathematical approach for calculating the power needed to operate PEVs.

$$R_{Trip,t} = kRL \quad \ldots (13)$$

where L is the voyage distance and κR is the energy consumption of PEVs per minute of transit. The smallest R_{min} and highest R_{max} of power left in each dispatched intervals should serve as constraints on R_t.

$$R_{out,min} \le R_t \le R_{out,max} \quad \ldots (14)$$

3 EO Algorithm Applied to Solve the WSPEV DEED Problem

The primary tenet of the EO approach is that mass and volume must be kept in balance. Here, the particles are solution representatives that act as searching agents whose own concentrations and positions are modified in accordance with the ideal solution[46,47]. To enhance the exploration as well as the exploitation phases, a generation rate term is incorporated. In the following section, the expression that governs the mechanism of mass balance is described:

$$V\frac{dC}{dt} = (C_{eqs} - C) + G \quad \ldots (15)$$

The concentration at equilibrium is represented by C_{eqs}, the internal concentration by C, and the mass generation rate by G, where VdC/dt is mass change ratio. The concentration after integration looks like this:

$$C = C_{eq} + (C_0 - C_{eq})e^{\tau(t_0 - t)} - \frac{G}{Q}\left[e^{\tau(t_0 - t)} - 1\right] \quad \ldots (16)$$

The beginning content is C_0, the start time is t_0, and the rate of change is Q/V. The first term is selected at random to be associated with the equilibrium pool. Exploration is linked to the second phrase. The search agents' pursuit of new areas is sometimes linked to exploration. Generation rate, or exploiters, is the third word. Each search agent's location is established using the following equation.

$$C_i^0 = C_{low} + u \times (C_{high} - C_{low}) \quad \ldots (17)$$

More detailed and complete step-by-step process for using the EO approach to solve the WSPEV DEELD problem while accounting for additional constraints and the inclusion of PEV load in the total load demand have been given in Fig. 1.

4 Results and Discussion

Several tests were conducted on different test systems in order to evaluate the effectiveness and feasibility of the proposed WSPEV DEELD system. A proposal with 10 and 20 thermal generating units has been implemented for the WSPEV DEELD system. renewable. The MATLAB 2021a program was used to conduct simulations on a computer with a core i5, 4th Gen CPU, and 4 GB RAM. Ninja supplies the thermal characteristics for this 10-unit system, wind units, solar plants, and PEVs. After 50 trial runs, the results of the 5000 iterations of the simulation were recorded. The important parameters are as follows: $\vartheta_c = 0.3$, $\vartheta_D = 0.3$, $C_{W,j} = 50$, $K_p = 75$, $K_{r,wd} = 0.85$. The Nissan Leaf, which has a 24 kWh battery and uses 0.15 kWh/km to accomplish the needed driving, has been used as a case study for PEVs. The dispatch window's temporal horizon is set at 24 hours. With v_{in}, v_{rated}, and v_{out} values of 3 m/s, 15 m/s, and 45 m/s, respectively, the rated capacities for solar and wind farms are 2 MW and 40 MW[49,50]. The values of w_u and w_d are as follows: 0.2 and 0.3.

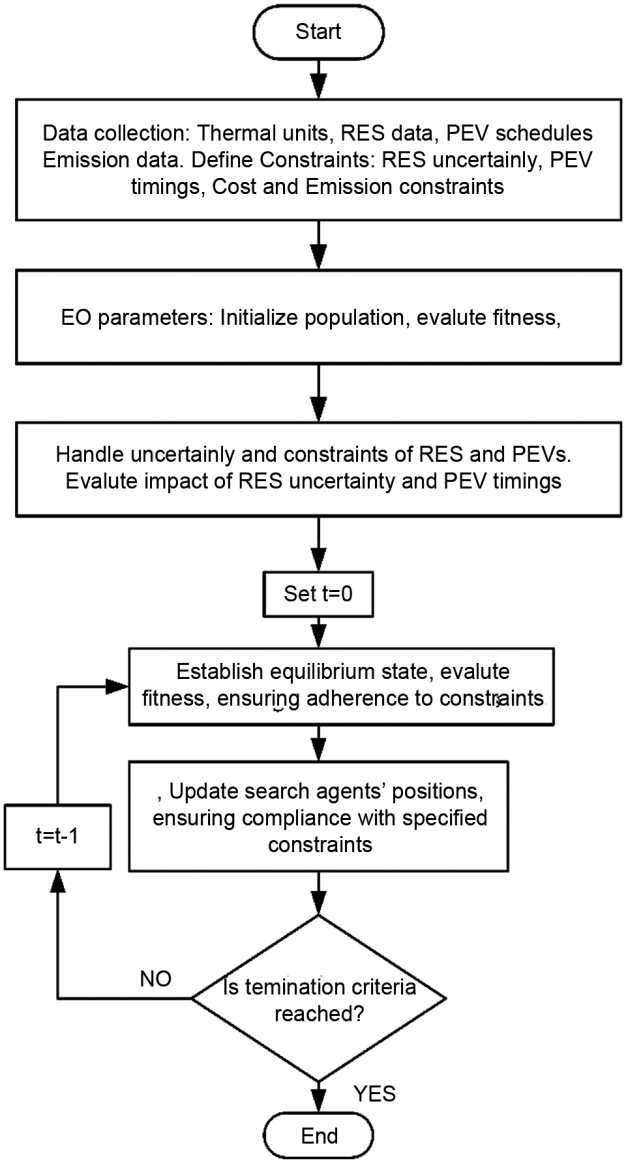

Fig. 1 — The EO solution's process flow diagram for the WSPEV DEED issue

4.1 Test System 1: The integration of 10 Thermal Generating Units with PEVs

A configuration including 10 thermal generating units and PEVs was used to assess the effectiveness of the proposed WSPEV DEELD model. The best compromise options for the first test system that came from using the EO method are shown in Table 1. PEVs are planned for off-peak times, which are, respectively, 22:00–6:00, 15:00–16:00, and 18:00. During specified periods, PEVs are supposed to be charged. As a result, the WSPEV DEELD model's dynamic features are fully used to facilitate PEV charging and discharging. The overall fuel cost is about $23,07,439.73, and the total emissions resulting from the EO algorithm are 2,42,216.21 tons. Figure 2 graphically displays the resultant energy for every unit and PEVs produced by the EO algorithm. After 50 iterations, Table 2 compares the best outcomes for lowering emissions, total fuel cost, and arriving at an agreement on compromise using the EO algorithm. The trade-off curve generated by the EO method for test system 1 is also shown in Fig. 3.

4.1.1 Tuning of EO Parameter for Case 1

In order to enhance computation efficiency and achieve the best performance, precise calibration of the EO algorithm parameters of GP, GCP, GP1, and GP2 is critical. The main objective is to determine parameter values for each test system that collectively minimize fuel cost and emissions. For methodological consistency, a parameter is changed while the others are held constant. In particular, GP and GCP are experimented within the range of 0.1 to 0.9 across various phases, while GP1 and GP2 are investigated within the ranges of 0.3 to 0.55 and 0.45 to 0.75, respectively. An experimental setup of 50 trials is used, with several independent runs performed to identify the best configurations providing the least fuel cost and emission values. The results are given in Table 3. The results point out that systematic parameter tuning considerably improves solution quality with less convergence time. Among the tested parameter settings, the combination of GP = 0.60, GCP = 0.40, GP1 = 0.30, and GP2 = 0.70 yielded the best optimum solution with minimum fuel cost and emission.

4.2 Test system 2: 10 Thermal Generating Units with PEVs and RES

Table 4 gives output of applying EO to the DEELD issue with integration of RES and PEVs. According to the PEV charging schedule, charging takes place between 22:00 and 06:00 and 15:00 and 18:00, which are off-peak hours, while discharging takes place between 07:00 and 14:00 and 19:00 and 21:00. The solar units were fed between 8:00 and 19:00, and at 14:00, they produced a maximum of 33.83 MW. At 7:00, the wind units produced a maximum of 25.03 MW. Test System 2 results showed an emission of 235,297.04 tons and a fuel cost of about $2,272,900.84. This suggests that adding PEVs prevented 6,919.17 tons of emissions per day in comparison to the base scenario, which

Table 1 — Findings for test system 1 from the EO algorithm

Time	T1 (MW)	T2 (MW)	T3 (MW)	T4 (MW)	T5 (MW)	T6 (MW)	T7 (MW)	T8 (MW)	T9 (MW)	T10 (MW)	PEVs	Fuel cost ($)	Emission (Tonnes)
1	82.37	100.71	147.92	120.28	166.49	137.24	168.04	161.19	82.88	50.27	-163.16	65300.96	5246.86
2	76.27	120.83	172.07	115.99	221.75	187.31	124.11	167.22	49.27	52.44	-159.45	68764.35	6049.12
3	135.56	115.18	111.72	151.09	192.69	216.12	189.05	167.76	72.55	48.32	-127.76	74970.99	6698.19
4	119.16	135.22	181.98	166.60	225.59	195.21	191.66	163.34	90.86	54.91	-106.62	81207.17	7857.15
5	117.70	190.28	155.34	167.31	260.78	198.34	211.50	192.07	59.08	42.83	-103.64	85598.52	8973.36
6	166.11	142.83	185.72	179.19	260.63	172.97	208.43	194.62	147.33	52.30	-73.87	92623.32	9732.93
7	143.52	250.60	210.17	201.75	277.82	177.75	142.55	124.99	120.86	51.99	28.96	96271.42	9853.47
8	147.43	148.70	214.04	205.98	267.19	280.90	150.85	159.46	115.75	50.35	31.80	93585.30	10437.58
9	188.79	212.88	227.31	208.21	265.20	188.84	245.31	217.80	60.21	53.22	50.58	102331.92	12389.13
10	149.16	232.11	228.14	194.59	273.27	255.33	237.63	236.11	64.51	49.65	91.30	103823.05	13138.73
11	146.27	208.42	239.42	241.61	222.47	296.24	225.98	244.26	102.70	51.75	114.11	106282.62	13966.55
12	214.03	232.00	185.97	245.46	335.34	177.09	221.97	266.59	108.13	40.45	89.93	112610.45	14621.64
13	228.27	198.14	258.07	219.27	277.53	279.94	185.70	165.54	117.63	47.88	84.58	110594.05	13342.68
14	146.83	205.61	202.50	224.46	288.08	245.54	238.35	201.12	54.87	54.52	55.88	99995.18	12408.88
15	214.93	145.52	214.41	199.80	280.17	187.66	221.78	211.48	147.48	50.23	-87.65	102835.40	11875.32
16	158.08	150.76	177.09	183.51	264.88	264.37	82.34	240.53	127.05	53.39	-133.13	92250.35	10109.32
17	153.07	131.57	166.76	179.05	177.65	207.10	166.27	159.42	84.96	54.17	-121.52	80322.89	7244.90
18	173.78	197.65	168.24	170.76	311.60	248.09	215.60	135.47	90.90	40.22	-111.81	95992.49	10524.72
19	168.80	200.62	190.21	202.85	220.07	302.81	132.08	166.80	110.41	41.35	35.99	95961.13	10206.68
20	153.17	228.16	229.33	229.70	257.12	156.24	224.10	245.71	113.91	53.25	73.14	103380.20	12657.35
21	163.30	224.24	215.94	223.20	320.04	251.19	173.32	190.31	53.06	42.80	59.90	101725.43	12407.79
22	146.77	194.95	180.76	132.07	225.66	247.01	199.87	122.01	135.13	51.11	-6.59	90202.37	8693.93
23	127.23	142.05	155.55	186.06	216.70	175.70	179.59	181.60	78.08	47.17	-141.87	79816.73	7593.64
24	85.87	126.04	170.58	155.09	177.64	200.14	166.28	123.81	78.06	47.72	-188.96	71388.45	6186.31

Table 2 — Comparison of EO's findings with those of other algorithms for minimizing emissions, fuel costs, and best compromise for test systems 1 (F_C (x10^6)) and (F_M (x10^5 Tonnes))

Algorithms	EO		SaMODE LS		SaMODE		MOEA/D		2lb-MOPSO		NSGA-II		SPEA2	
	FC	FM	FC	FM	FC	FM	FC	FM	FC	FM	FC	FM	FC	FM
Minimize Fuel cost	2.28	2.45	2.39	2.78	2.46	2.82	2.48	2.77	2.45	2.91	2.50	2.68	2.51	2.64
Minimize emission	2.32	2.41	2.50	2.51	2.58	2.55	2.59	2.53	2.60	2.52	2.52	2.63	2.53	2.63
Compromise solution	2.30	2.42	2.43	2.60	2.50	2.62	2.51	2.61	2.50	2.64	2.51	2.66	2.51	2.64

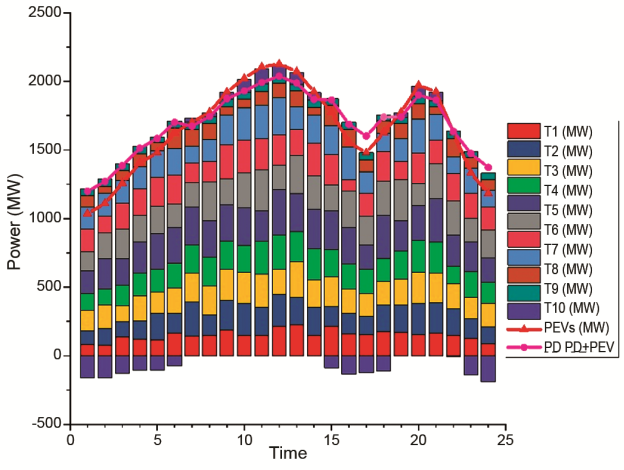

Fig. 2 — Display of all units' and PEVs' output power as determined by the EO algorithm in test system 1

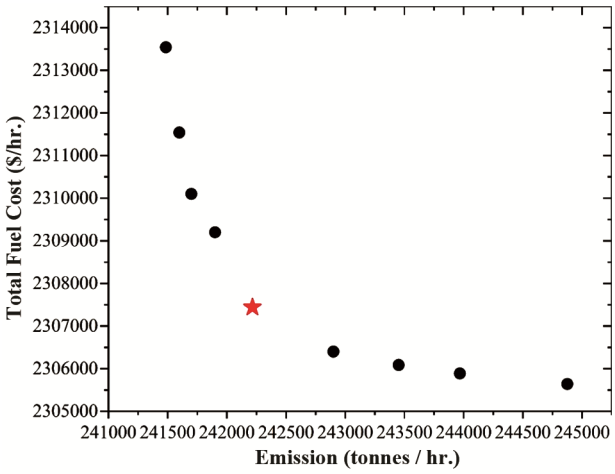

Fig. 3 — The EO algorithm's trade-off curve for test system 1

translates into a net reduction of 83,030.04 tons of emissions per year in the transportation and energy sectors.

Additionally, it reduced expenses by around $34,538.89 each day, which translates to an annual savings of about $414,466.68 to further lower operating costs in the transportation sector. Figure 4

Table 3 — Tuning of EO Parameters for Fuel Cost and Emissions

GP	GCP	GP1	GP2	Fuel Cost ($)	Emission (tons)
0.40	0.60	0.30	0.70	2,345,210.56	245,310.22
0.45	0.55	0.25	0.75	2,332,890.47	243,876.45
0.50	0.50	0.20	0.80	2,320,560.33	243,110.72
0.55	0.45	0.25	0.75	2,312,740.15	242,876.93
0.60	0.40	0.30	0.70	2,307,439.73	242,216.21
0.65	0.35	0.35	0.65	2,315,780.18	243,119.57
0.70	0.30	0.40	0.60	2,327,510.89	244,221.45
0.75	0.25	0.45	0.55	2,340,890.62	245,780.33
0.80	0.20	0.50	0.50	2,356,210.44	247,310.51
0.85	0.15	0.55	0.45	2,372,890.71	249,225.62

Table 4 — Outcomes of the EO algorithm for test system 2

Time	T1 (MW)	T2 (MW)	T3 (MW)	T4 (MW)	T5 (MW)	T6 (MW)	T7 (MW)
1	81.4965	117.5637	107.653	122.9658	173.7619	162.9855	167.6902
2	135.4184	106.5065	153.7292	124.2796	168.4249	164.5158	131.9628
3	149.9231	128.8432	168.7149	130.9129	224.1129	245.8388	123.5585
4	138.4413	198.3811	163.2917	140.1698	258.5181	218.6581	119.5746
5	170.2762	131.6702	253.7969	168.5967	243.7838	189.782	181.4819
6	152.5111	204.1829	201.9975	144.993	283.0205	198.1539	189.9491
7	186.9298	156.277	162.655	239.3742	314.7377	240.3136	148.9303
8	149.9492	133.1625	234.6326	181.9303	153.6431	295.9589	210.6052
9	163.5225	197.3323	229.1106	176.0599	322.3091	256.9941	243.083
10	180.9126	177.3257	253.6619	239.2463	330.0924	306.8091	138.1607
11	203.0478	197.918	261.493	183.1075	270.9803	333.4861	219.7577
12	178.7645	227.6859	275.1474	187.5421	329.4588	306.0704	229.8869
13	182.178	215.4978	280.716	234.2909	267.9451	267.3183	231.7325
14	147.6806	165.7125	194.1886	185.8451	274.5064	312.6041	184.2971
15	172.1687	182.2026	125.6382	196.8601	231.4083	151.9421	206.3448
16	136.7799	133.9897	175.085	177.8004	179.3878	196.5362	158.5506
17	127.6845	123.8255	171.7964	172.9737	174.7606	191.0702	118.5193
18	174.6078	212.4187	134.9771	141.7322	174.1584	175.6831	140.109
19	156.5896	135.3636	172.5047	188.8416	262.8668	250.1539	176.5507
20	153.927	150.7931	203.4032	163.6599	276.243	260.6182	244.8066
21	131.6552	230.7603	214.7638	122.7514	267.7643	292.7954	236.4417
22	79.5315	127.571	179.0925	181.0221	221.8173	245.1915	172.6274
23	142.2209	152.4797	111.267	121.0715	172.8834	180.7717	138.2733
24	95.6196	131.8189	134.5892	120.3471	191.3668	193.2523	129.258
T8 (MW)	T9 (MW)	T10 (MW)	Solar Output	Wind Output	PEV	Fuel cost ($)	Emission (Ton)
115.6459	53.0203	46.4071	0	15.1343	-128.3276	62405.72	4720.03
158.8955	83.8643	40.2429	0	10.9049	-168.749	69238.84	5407.352
162.7139	52.9945	45.9974	0	3.2473	-178.8574	77700.62	7133.153
205.2606	96.8404	48.8944	0	1.8966	-183.9239	87069.09	8393.759
158.5044	112.8649	45.133	0	2.9657	-178.8574	89862.71	9596.774
248.0637	99.9132	43.3451	0	0.3041	-138.436	95701.18	10793.06
131.848	116.1725	53.672	3.61	0.0106	-52.5268	96307.9	10569.65
218.0728	97.621	47.7444	11.7185	0.0128	40.9514	91626.51	10857.9
125.8714	91.5708	54.4564	20.1411	0.0735	43.4785	100965	12216.91
200.3053	77.7433	39.4726	26.9715	0.2436	51.0598	105407.3	14006.73
237.9407	58.2113	52.0577	28.5491	0.8126	58.6412	109695.6	14710.02
161.0069	134.771	28.4762	27.7082	2.0614	38.4243	113231.3	15106.36
89.9436	192.2241	51.2537	26.7671	3.8177	28.3159	113073.8	14421.48

(*contd.*)

Table 4 — Outcomes of the EO algorithm for test system 2 (*contd.*)

Time	T1 (MW)	T2 (MW)	T3 (MW)	T4 (MW)	T5 (MW)	T6 (MW)	T7 (MW)
247.1664	94.5805	54.7787	22.7067	6.5583	33.3701	98685.73	12135.87
250.2306	137.8571	51.4875	16.2826	10.1019	43.4785	93541.11	9918.072
209.0936	61.3785	51.2583	7.3084	13.2454	53.587	79359.57	7654.196
163.3863	87.2478	49.4858	0.219	15.1303	83.8999	74914.18	6444.856
140.4538	139.2507	54.3093	0	15.9645	124.3336	85598.53	6834.14
86.3647	118.1177	50.2367	0	16.1799	162.2278	86952.08	8743.92
227.7968	82.5979	52.1243	0	16.5364	139.4962	95790.77	11677.43
144.8446	93.4364	52.0969	0	17.4109	119.2794	97515.86	11196.77
189.9035	82.7767	51.8365	0	17.7733	78.858	80296.67	8390.4
127.0914	111.1757	54.8154	0	16.9066	3.0449	73318.87	5350.85
84.0387	108.3706	52.4088	0	15.6786	-72.7436	68352.08	5099.569

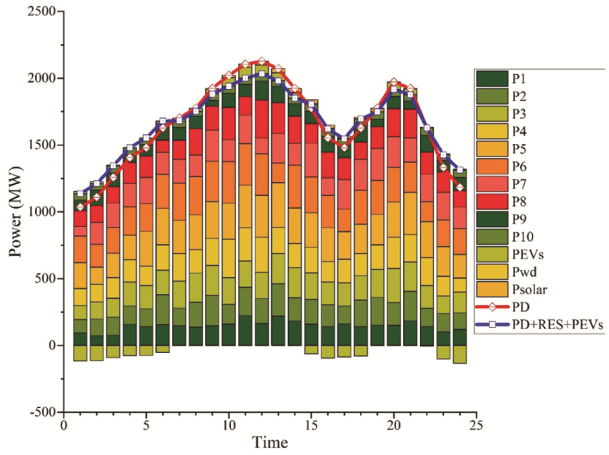

Fig. 4 — Display of all units' and PEVs' output power as determined by the EO algorithm in test system 2

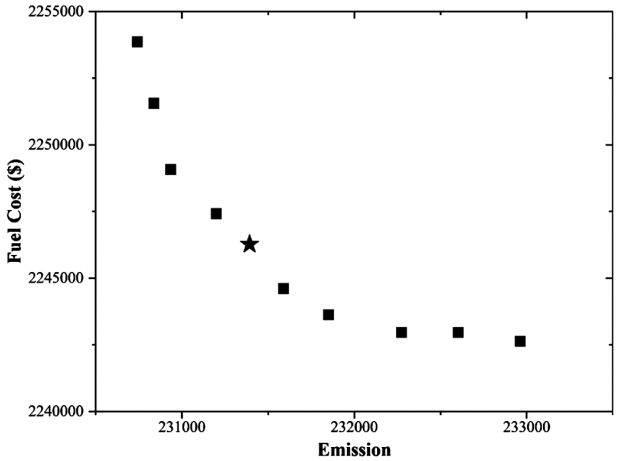

Fig. 5 — The EO algorithm's trade-off curve for test system 2

shows the output power in visual form for all units and PEVs in test system 2, as optimized by the EO algorithm. The compromise graph for test system 2, which was obtained using the EO method, is also shown in Fig. 5. It emphasizes the equilibrium among cost and emissions.

4.3 Test system 3: The integration of 20 Thermal Generating Units with PEVs

In the simulation test of Test System 3 of 20 thermal generating units inter- acting with a very complex interaction with 1,20,000 PEVs. The results, which are carefully reported in Table 5, detail the finegrained power distribution between thermal units and, consequently, the ability of the algorithm to handle various forms of energy sources. Table 6 captures a comparison of results for test system 3. Meanwhile, Fig. 6 graphically presents the tradeoff curve due to the EO algorithm, giving an idea into how it can compromise conflicting objectives. The discussion of these results goes into the subtleties of the system dynamics, bringing forth the urgency in reducing the UE and OE errors, establishing PEV behavior to be able to calculate power generation more accurately, and assessing the efficiency and trade-offs achieved by the EO algorithm as a whole. Such exhaustive investigation opens vast implications toward power system optimization to design future sustainable energy planning and to formulate proper management strategies.

4.4 Test system 4: 20 Thermal Generating Units with PEVs and RES

The outcome of applying the EO for Test System 4 to solve the WSPEV DEELD issue with integrated RES and PEVs is taken into consideration. When the peak power demand was declining at 9:00, the highest output of solar units was about 56.96 MW at 11:00 and the greatest generation of wind units was approximately 97.56 MW at 14:00. At this time, the generation happened between 1:00 and 7:00 and also at 24:00, whereas the emission happened between 8:00 and 23:00. Based on the data collected, 58,168.60 tons of emissions were produced at a cost of around $1,361,543.64. As a result, it has decreased the power plants' daily emissions by 77,145.56129 tons, or 1,609,753.3165 tons annually. Additionally, it cut the daily cost of gasoline by around $138,236.90. Table 7 displays output for test system 4,

Table 5 — Findings for test system 3 from the EO algorithm

Time	T1 (MW)	T2 (MW)	T3 (MW)	T4 (MW)	T5 (MW)	T6 (MW)	T7 (MW)	T8 (MW)	T9 (MW)	T10 (MW)	T11 (MW)
1	1886.03	204.84	87.29	63.73	34.46	132.36	44.91	129.88	61.38	169.83	110.04
2	1831.28	189.94	124.46	47.36	168.29	97.96	69.56	136.34	94.37	117.13	18.23
3	1817.61	195.26	106.18	43.1	59.38	99.85	68.86	120.1	75.51	151.13	25.88
4	1810.79	184.84	107.25	36.23	109.55	96.43	20.36	147.84	80.88	130.14	25.42
5	1817.62	181.94	103.93	52.01	58.17	108.58	50.46	136.99	66.91	85.99	107.54
6	1872.33	163.52	117.96	47.5	102.1	155.01	16.21	156.19	39.13	121.68	81.08
7	1988.61	214.48	88.25	104.14	49.84	94.5	98.5	174.26	130.61	113.43	77.73
8	2115.21	207.16	104.86	89.15	117.02	166.58	89.08	153.08	85.11	160.91	122.49
9	2118.63	190.39	117.06	105.8	163.77	103.19	46.49	166.37	108.56	155.74	64.77
10	2128.91	191.18	96.25	82.06	97.34	157.16	82.63	79.04	143.5	190.18	100.47
11	2139.19	200.61	101.49	83.68	81.2	140.27	80.88	184.9	69.58	164.82	117.13
12	2111.77	226.1	128.15	69.27	193.56	154.88	29.11	102.77	103.13	179.77	71.85
13	2098.09	198.33	74.21	84.11	82.84	145.24	89.5	181.23	108.33	177.71	132.17
14	2104.94	187.91	131.01	76.04	102.29	139.42	45.78	165.77	72.35	179.08	119.96
15	2118.63	159.61	112.4	102.79	134.96	166.12	50.64	89.12	82.2	147.38	70.7
16	2132.32	202.46	129.23	70.35	113.75	159.47	58.85	168.77	36.88	154.38	108.41
17	2173.46	189.73	70.89	91.82	149.18	77.92	59.5	181.5	139.06	204.61	158.31
18	2228.31	217.07	102.77	50.26	134.45	96.66	181.83	191.99	89.43	164.34	108.43
19	2279.76	183.13	119.81	104.08	174.75	184.41	133.18	186.83	147.27	124.46	76.51
20	2248.88	200.8	94.36	117.74	134.05	134.31	83.85	184.35	114.8	102.04	96.76
21	2221.45	204.51	100.02	123.15	169.06	76.9	130.44	157.99	64.19	185.85	113.14
22	2166.6	198.43	114.51	114.89	65.14	144.16	37.58	178.39	127.41	138.72	145.55
23	2063.88	218.41	115.43	89.9	129.8	136.58	35.32	166.34	86.51	130.94	116.84
24	1961.25	205.59	100.52	98.95	105.13	142.43	21.89	159.09	81.45	113.8	61.14
T12 (MW)	T13 (MW)	T14 (MW)	T15 (MW)	T16 (MW)	T17 (MW)	T18 (MW)	T19 (MW)	T20 (MW)	PEV (MW)	Cost ($)	Emission (Ton)
196.03	191.28	91.53	132.97	27.73	29.89	26.58	41.24	59.59	50.47	48859.54	2829.36
190.06	214.68	84.11	82.94	26.58	16	22.29	40.86	48.79	41.32	47846.31	2721.05
195.23	203.73	155.21	130.22	22.94	25.41	24.4	46.85	30.89	37.48	47488.78	2585.87
190.54	183.46	163.33	148.36	25.04	22.39	23.2	48.66	32.45	34.41	47412.83	2469.98
193.66	193.14	118.96	131.28	19.97	29.22	14.46	49.01	61.61	53.8	47517.94	2429.03
198.82	195.99	145.11	78.4	25.75	27.52	18.18	61.87	67.84	52.48	48586.47	2783.77
192.33	210.86	181.14	21.51	25.02	18.59	15.54	76.25	52.09	49.53	50993.49	3138.08
209.59	177.32	126.57	61.77	34.91	25.76	28.58	62.4	45.31	47.55	53450.5	3219.84
174.52	193.61	95.37	154.19	26.99	30.26	24.22	51.67	74.03	71.64	53599.47	3318.54
188.5	211.97	123.67	139.75	23.95	26.22	24.72	38.99	65.09	66.24	53813.62	3172.42
190.21	201.81	144.23	147	28.49	28.21	16.13	30.27	63.41	64.86	53879	3170.67
208.28	203.54	176.13	39.56	45.8	22.88	29.98	22.95	52.87	51.2	53388.97	3227.9
179.63	205.92	139.2	82.42	21.2	31.88	32.7	27.88	53.72	49.87	53113.62	3087.63
198.85	212.91	155.98	80.57	15.3	22.24	30.13	54.21	58.74	56.41	53174.31	3240.72
195.95	220.63	145.84	165.5	24.36	39.56	37.19	73.68	41.98	58.03	53578.03	3531.61
186.67	215.52	162.96	90.05	36.37	16.94	40.6	67.59	47.53	65.52	53719.25	3687.85
205.88	201.92	185.33	46.16	29.9	25.64	28.58	36.74	41.8	48.96	54729.37	3554.25
179.92	216.7	143.77	89.37	37.5	24.76	17.63	71.08	50.82	59.53	55700.64	3726.94
216.58	208.67	84.08	55.89	37.6	32.62	36.43	51.46	43.15	78.85	56888.44	4181.49
187.6	200.18	184.34	155.49	40.84	22.94	28.46	22.7	72.89	70.37	56172.58	3704.69
195.54	205	159.34	108.07	17.86	39.64	25.27	43.17	45.12	57.19	55631.26	3544.74
205.81	216.33	163.47	34.38	32.2	28.51	38.09	56.11	66.63	60.27	54467.82	3799.76
173.92	203.04	55.68	158.01	34.37	19.85	25.14	52.78	52.94	62.07	52475.77	3212.19
175.7	205.09	140.11	137.2	25.67	16.37	28.14	42.3	64.07	36.6	50378.57	2807.17

Table 6 — Comparison of test system 3's EO algorithm results with those of other algorithms

Methods	Total cost ($)	Total emission (Tonnes)
EO	1382369	77145.56
SaMODE LS	1407896	77415.63
SaMODE	1458874	78987.51
MOEA/D	1469854	79412.88
2lb-MOPSO	1469912	80785.54
NSGA-II	1474521	81852.21
SPEA2	1485632	81145.65

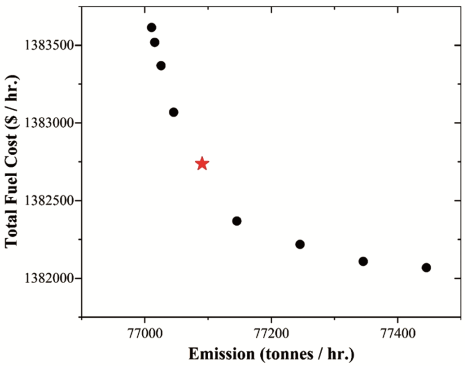

Fig. 6 — The test system 3 trade-off curve produced by the EO algorithm

Table 7 — Findings for test system 4 from the EO algorithm

Time	P1 (MW)	P2 (MW)	P3 (MW)	P4 (MW)	P5 (MW)	P6 (MW)	P7 (MW)	P8 MW)	P9 MW)	P10 MW)	P11 (MW)	P12 (MW)
1	165.424	81.1066	38.7555	111.0141	118.6893	62.6264	112.9649	107.3365	161.2392	144.6108	189.6307	181.8003
2	179.4774	73.0238	52.3433	83.5242	110.659	35.0513	160.5933	54.8901	145.992	62.9928	205.3637	196.8604
3	179.4688	84.5236	39.3964	61.6364	97.9484	23.7572	128.0348	89.6635	135.947	131.0037	194.5406	191.0901
4	194.9294	25.6967	52.0733	70.8463	148.0521	32.4731	153.5287	49.6211	163.5208	36.7534	169.1989	213.1536
5	194.2939	105.2271	12.8065	63.9943	119.7098	77.2041	146.0093	45.4021	100.4797	63.4947	189.626	193.3242
6	194.8015	58.193	40.9091	22.8933	82.8838	31.7706	176.5947	96.4369	164.999	71.732	180.4376	200.556
7	173.755	105.6555	75.4043	135.4331	120.2421	60.466	119.9845	76.6741	134.7119	113.576	192.4028	194.0608
8	197.1424	126.0066	108.3635	90.2332	135.1303	54.3345	78.2394	86.2165	185.9954	62.8857	212.9037	219.7355
9	163.4701	132.3574	88.3404	77.8569	168.4232	64.4822	97.6936	146.0045	118.7675	122.0312	205.3754	194.9102
10	196.1366	118.7907	99.8233	97.8701	117.2364	34.7187	58.423	74.3242	181.8194	140.9553	196.3245	199.2594
11	207	100.8436	37.6733	97.9153	160.7286	32.3608	164.3263	119.5129	127.333	151.8303	139.5013	208.5148
12	190.0809	111.589	57.6888	104.8049	148.6356	121.4049	182.7343	84.9093	177.8507	15.9394	191.3602	199.5753
13	199.7795	81.8458	97.1327	98.4779	76.9743	140.8572	165.9303	99.144	177.609	31.1982	182.6993	218.8269
14	187.6053	105.6511	31.6614	128.2415	156.8601	98.1295	169.9108	42.3008	95.7286	173.075	161.2072	165.065
15	185.2546	118.912	71.7083	186.7115	148.9254	32.0464	211.6245	55.3226	83.3064	109.3835	221.7964	198.6734
16	204.3915	131.5964	74.9419	66.2053	148.1724	95.7055	121.1874	141.8999	137.1111	104.0407	190.7806	194.2383
17	186.8151	99.246	91.6549	133.78	141.2333	38.0206	160.3463	152.2823	148.7682	146.0842	200.3604	154.3943
18	196.485	106.3944	49.5351	125.3824	149.6725	97.2252	129.2637	118.1237	175.3977	111.8893	193.4122	205.0586
19	186.6709	127.5919	84.1694	165.0284	147.0231	113.8168	142.3896	93.9223	159.7134	119.1673	213.7685	198.9347
20	205.0832	116.9439	129.9842	143.0817	144.0962	165.5038	71.4635	74.7754	176.3469	161.8055	206.3217	181.5338
21	178.3296	99.425	95.5399	139.6489	122.042	43.0877	179.7058	166.8481	156.9454	173.067	175.2279	187.3535
22	165.9665	119.9829	97.0291	130.644	118.5154	82.6391	193.5673	73.0135	112.9641	142.777	193.9035	192.6213
23	194.9991	99.8533	80.3875	121.5241	107.7576	44.7022	164.4639	26.0919	129.7387	157.7098	189.3003	207.6686
24	185.7017	98.0534	98.6068	111.9725	135.3712	72.4693	142.5875	101.1094	74.5678	74.1021	187.5832	181.792
P13 (MW)	P14 MW)	P15 (MW)	P16 MW)	P17 (MW)	P18 (MW)	P19 (MW)	P20 (MW)	Solar Output (MW)	Wind Output (MW)	PEV MW)	Fuel cost ($)	Emission (Ton)
82.0163	128.1969	25.7006	34.5742	19.7588	24.0415	36.8128	31.463	0	3.751	-56.9111	48439.8099	237.5831
150.2506	72.6226	25.3411	14.1581	17.0431	54.3716	68.06	30.8912	0	5.5295	-74.8389	47015.0332	254.1911
122.5234	97.6202	30.101	23.1336	21.8212	21.0215	55.8266	46.6491	0	7.7309	-79.3208	46709.4621	238.223
115.3805	105.4339	23.1753	10.5667	19.1179	64.8869	67.7301	49.2008	0	10.3076	-81.5618	46521.2125	265.1276
121.1666	154.5276	12.0562	14.4372	21.4182	55.6906	48.8071	31.5428	0	12.2322	-79.3208	46600.5424	232.184
153.6671	96.9502	32.0163	20.5736	27.1823	62.4396	67.9613	49.7689	0	13.1176	-61.3931	47807.3927	290.3735
160.2389	115.1089	35.8171	19.5196	21.451	38.9959	35.5289	37.1945	0	12.3515	-23.2967	50517.7417	258.8505
129.5325	170.9024	32.0743	24.4125	21.0801	49.0607	54.2935	57.8917	15.8089	10.7944	18.1611	53068.8631	347.8461
160.7884	49.268	37.3507	39.4693	23.3956	67.8951	52.3039	71.1353	41.6665	3.9481	19.2816	52891.216	346.4192
129.0195	192.967	32.9222	18.5244	33.8911	15.1281	63.4719	76.4395	59.6965	0.92	22.6431	52854.3058	349.5723

(*contd.*)

Table 7 — Findings for test system 4 from the EO algorithm (*contd.*)

Time	P1 (MW)	P2 (MW)	P3 (MW)	P4 (MW)	P5 (MW)	P6 (MW)	P7 (MW)	P8 MW)	P9 MW)	P10 MW)	P11 (MW)	P12 (MW)
167.4584	161.4193	16.0793	30.5816	22.0872	29.6433	62.388	39.2367	70.059	3.9019	26.0045	52716.4621	299.7465
134.6182	81.8509	29.6564	23.6899	26.4574	50.0512	64.1427	44.2696	74.7352	3.073	17.0407	51964.6361	309.5634
194.4882	81.9259	36.3712	23.2642	15.7343	24.2354	36.6972	43.4528	75.3102	1.5485	12.5587	51757.2714	315.4262
110.1441	177.7531	20.1397	23.0706	28.5908	52.3922	60.2916	51.5226	71.0246	0.951	14.7997	52100.8881	280.9346
100.1947	103.5608	10.4619	27.6131	20.0997	72.2848	50.0526	56.037	61.3381	1.6304	19.2816	52470.5894	350.896
171.1624	131.5984	29.2521	18.042	22.9286	31.6304	41.8933	37.9808	45.8723	1.9275	23.7636	53081.9447	291.1326
134.9061	142.645	18.9127	26.5034	30.1138	63.3082	48.726	46.0737	23.2903	2.0216	37.2094	54578.1251	295
170.5577	177.8247	26.2424	23.5988	34.2292	63.8993	43.7542	51.4732	0.8731	1.7735	55.1371	56119.4613	341.6938
156.2301	119.8645	38.2344	37.0123	29.9654	68.2218	45.609	61.5124	0	1.9091	71.9443	57284.654	384.289
157.3447	80.8119	32.7518	40.907	11.8535	70.7939	40.7372	58.7937	0	4.6017	61.86	56766.9406	377.6991
168.469	92.1484	19.7444	35.2607	22.629	77.1751	43.6999	56.772	0	11.1242	52.8961	55981.7986	331.3441
162.7546	150.8082	14.1774	25.9288	23.1174	62.212	48.6363	54.1092	0	16.2962	34.9683	54514.9519	299.2358
130.6132	151.8342	11.7947	24.5054	32.5108	66.1959	65.7039	35.7401	0	21.3611	1.3539	51993.8592	306.5872
104.9848	106.5632	28.4504	27.6514	29.1041	28.9982	68.066	62.2	0	27.4172	-32.2605	49653.5544	268.718

Table 8 — Comparison of the EO algorithm's results with those of other algorithms for test system 4

Methods	Total cost	Total emission
EO	1361544	58168.6
SaMODE\LS	1374141	59562.77
SaMODE	1374512	59987.11
MOEA/D	1374951	60524.74
2lb-MOPSO	1386785	61452.21
NSGA-II	1397552	62785.95
SPEA2	1408415	63485.99

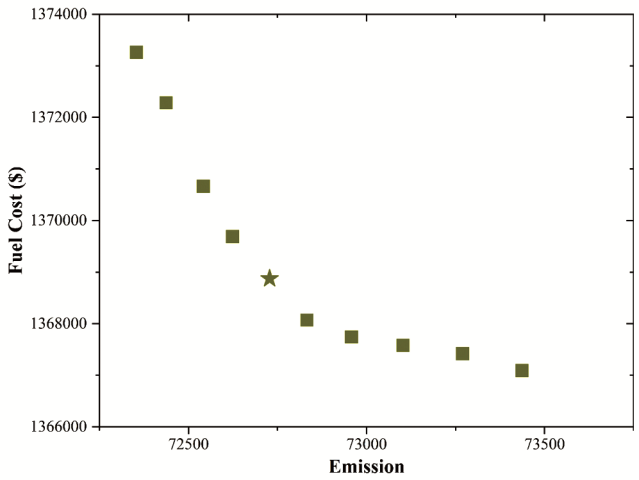

Fig. 7 — The test system 4 trade-off curve produced by the EO algorithm

demonstrating the best power dispatch and emission performance. Table 8 presents a comparison of these outcomes with those of other optimization algorithms, highlighting the EO algorithm's better performance in terms of minimizing costs and reducing emissions. Figure 7 shows the trade-off curve for test system 4, which was produced by the EO algorithm and emphasizes the harmony between environmental and economic goals. This comparison demonstrates how well the EO algorithm works to resolve challenging load dispatch issues.

5 Conclusion

A revolutionary WSPEV DEELD model is introduced by this creative method of integrating PEVs, wind and solar power systems, and heat producing units. This model's primary focus is on optimizing fuel costs and pollutant gas emissions in a 24-hour period by using wind, solar, and PEV resources. The paper strongly suggests utilizing the EO approach to solve the WSPEV DEELD issue. The methodology is renowned for its amazing exploration and exploitation capabilities, which provide a quicker approach to the solution space. The suggested approach's resilience properties are confirmed by simulations on a variety of test systems based on 10 and 20 thermal units. The performance results of the EO algorithm reveal its consistency in superiority over the base, with better dispatch solutions for less overall cost and emissions while simultaneously relieving the costs of UE/OE through the WSPEV DEELD model. Importantly, this work represents the first attempt to take into consideration 10 and 20 thermal generating units in addition to PEVs and RES considering real data. Consideration of PEV arrival/departure times, waiting periods, in addition to the UE/OE costs of RES within the DEED problem culminated into successfully realizing the modes of PEV charging and discharging as well signifies the adequacy of the model. Some further work may thus

involve taking this model forward to include more units or optimizing it better towards efficiency and applicability.

Nomenclature

a_i, b_i, c_i, e_i, f_i	Cost coefficients of the *ith* thermal generator	$S_{rad,stc}$	Solar irradiance under standard test conditions
N	Total number of thermal generating units	$S_{P,stc}$	Solar output power under standard test conditions
T_i	Output power of the *ith* thermal unit (MW)	γ	Temperature coefficient (%/ C)
Wp, Sp	Combined wind–solar generation power (MW)	T_{cell}	Temperature of a photovoltaic (PV) cell
Cw	Operating cost of wind generation ($/h)	$T_{cell,stc}$	PV cell temperature under standard test conditions
Nw, Ns	Number of wind and solar units	NOT	Nominal operating temperature of the PV cell
Bidl	Bidding price of the *lth* solar unit	Nsc, Npc	Series and parallel configuration of solar cells
TL	Transmission network losses	μ, σ	Mean value and standard deviation
TD	System load demand	Ik	Input constant
Bij, B0i, B00	Coefficients of transmission loss formula	Se	Total electrical generation (wind + solar + thermal)
T_i^{min}, T_i^{max}	Lower and upper operating limits of the *ith* unit	zl	Random variable representing input uncertainty
Shp, Scp	Weibull distribution parameters	Qi(t), Qj(t)	Charges associated with the *ith* and *jth* particle
v, vr	Instantaneous and rated wind speed	Ppv,av, Ppv,kt	Available and predicted output power of the *kth* solar unit
vin, vout	Cut-in and cut-out wind speeds	Cpv	Cost coefficient of the *kth* PV unit
Wp, Wpt	Instantaneous and rated wind power	Rij(t)	Euclidean distance between two particles
ω, ψ	Beta distribution parameters	PWj,av, PWd,jt	Available and forecasted power of the *jth* wind unit
Γ	Gamma function parameters	Kp,wd, Kr,wd	Penalty coefficients for wind power under/overestimation
Srad (t)	Solar radiation intensity at time *t*	αiT, βiT, γiT, ζiT, λiT	Emission coefficients of the *ith* unit

References

1 Zou D, Ma L, Li C & Ouyang H, *Engg Appl Artif Intell*, 138 (2024)109293.
2 Soni J & Bhattacharjee K, *Environ Develop Sustain,* (2023b).
3 Soni J & Bhattacharjee K, *Engg Opt* (2024b).
4 Ma H, Yang Z, You P & Fei M, *Energy*, 135 (2017)101
5 Verma D, Soni J, Kalathia D & Bhattacharjee K, *Intl J Swarm Intell Res*, 13(1) (2022) 1
6 Bhattacharjee K, Shah K & Soni J, *Electr Power Components Syst*, 49(11) (2022) 1034
7 Shah K, Soni J & Bhattacharjee K, *Int J Swarm Intell Res*, 14(1) (2023) 1
8 Soni J & Bhattacharjee K, Soft computing applications in modern power and energy systems: Select proceedings of eprec, *Springer Nature Singapore,* (2022) 175
9 Soni J & Bhattacharjee K, *Int J Ambient Energy*, 44(1) (2023a) 2386
10 Qiao B, Feng Z, Zhu Z, Yan L, Qu B, Chai X, Huan J, *Swarm Evolution Comput*, 98 (2025) 102096
11 Zou D, Ma L, Li F, Ouyang H & Shao Y, *Comp Ind Engg*, 203 (2025) 110969
12 Wu P, Zou D, Zhang G & Liu H, *Energy Sci Engg* , 12 (4) (2024) 1699
13 Bhattacharjee K, Bhattacharya A & Nee Dey S H, *Int J Electr Power Energy Syst*, 73(2015) 830
14 Basu M, *Int J Electr Power Energy Syst*, 82(2016) 213
15 Fauziyah N & Hariyanto N, *IEEE 3rd international conference in power engineering applications*, (2023) 163
16 Thorat A, Korachgaon I & Mulla A, *Int J Electr Engg Tech*, 12(6) (2021) 19
17 Qu B, Qiao B, Zhu Y, Jiao Y, Xiao J & Wang X, *International conference on swarm intelligence,* (2017) 31
18 Chen F, Zhou J, Wang C, Li C & Lu P, *Energy*, 121 (2017) 276
19 Qu B, Qiao B, Zhu Y, Liang J & Wang L *Energies*, 10 (12) (2017) 1991

20 Yan L, Zhu Z, Kang X, Qu B, Qiao B, Huan J & Chai X, *Energies*, 15(14) (2022) 4942

21 Zou D, Li S, Xuan K, Ouyan H, *Comp Ind Engg*, (2022a) 108717

22 Qiao B & Liu J, *International conference on bio-inspired computing: Theories and applications,* (2019) 65

23 Chen J, Liu X & Karam I, Environ Dev Sustain Springer, 1 (2024).

24 Moghaddam Z, Ahmad I, Habibi D & Masoum M A, *IEEE Transactions on Transportation Electrification*, 5(1) (2019) 226.

25 Yao W, Zhao J, Wen F, Xue Y & Ledwich G, *IEEE Transactions on Power Systems*, 28(3) (2013) 2768

26 Soni J & Bhattacharjee K, *Intl J Swarm Intell Res*, 13(1) (2022) 1

27 Kang Q, Feng S, Zhou M, Ammari A C & Sedraoui K, *IEEE Trans Intell Transp Syst*, 18(9) (2017) 2557

28 Liu G, Zhu Y L & Jiang W, *IET Gener, Trans Distrib*, 12 (17) (2018) 3972

29 Goel R & Maini R, *J Comp Sci*, 25 (2018)28

30 Nourianfar H & Abdi H, *Res Technol Electr Ind*, 1(1) (2022) 46

31 Zhang Y, Le J, Liao X, Zheng F, Liu K & An X, *Renew energy* , 128 (2018b) 91.

32 Zhao J, Wen F, Dong Z Y, Xue Y & Wong K P, *IEEE Transactions on industrial informatics*, 8(4) (2012) 889

33 Behera S, Behera S & Barisal A K, *Int J Ambient Energy*, 43(1) (2022) 4683

34 Al-Bahrani L T, Horan B, Seyedmahmoudian M & Stojcevski A *Energy*, 195(2020) 116946

35 Basu M, *Renew Energy Focus*, 28(2019) 11.

36 Bhattacharjee K, Bhattacharya A & Nee Dey S H, *Int J Electr Power Energy Syst*, 63(2014) 145.

37 Faramarzi A, Heidarinejad M, Stephens B & Mirjalili S, *Knowl- Based Syst*, 191(2020) 105190.

38 Galus M D & Andersson G, *IEEE Energy 2030 conference* (2008)1.

39 Gao J & You F, *Comp Chem Eng*, 122(2019) 31.

40 Mei P, Wu L, Zhang H & Liu Z, *Energies*, 12(20) (2019) 3847.

41 Qiao B & Liu J (2020). *Bio-inspired computing: Theories and applications: 14th international conference, bic-ta 2019, zhengzhou, china, november 22–25, 2019, revised selected papers, part i 14* (65–76).

42 Qiao B, Liu J & Huan J, *Soft Computing*, 26(22) (2022) 12833.

43 Rajani B & Sekhar D C, *Int Trans Electr Energy Syst*, 31(6) (2021) e12905.

44 Shevchenko H, *Baltic J Economic Studies*, 3(1) (2017) 109.

45 Soni J & Bhattacharjee, K, *Multiscale Multidisciplinary Modeling, Experiments Design*, (2024a) 1.

46 Soni J & Bhattacharjee K, *Electr Engg*, (2024c) 1.

47 Sun S, Yang Q, Ma J, Ferr´e A J & Yan W, *Renew Energy*, 150 (2020) 356.

48 Zhang Y, Le J, Liao X, Zheng F, Liu K & An X, *Renew energy* , 128(2018a) 91.

49 Zou D, Li S, Xuan K & Ouyang H, *Comp Ind Engg*, 173 (2022b) 108717.

50 Zou Y, Zhao J, Ding D, Miao F & Sobhan B, *Sustain Cities Society*, 67 (2021) 102722